Pattern competition for the sequential bifurcations approach (SBA) to turbulence in the co-rotating Taylor–Couette system: Quinary states

T. Akinaga,[1,*] S. C. Generalis,[2,] and E. C. Aifantis[3,***]**

(Submitted by A. M. Elizarov)

[1] *Faculty of Engineering Science, Akita University, 1-1 Tegata-Gakuen Machi, 010-8502, Akita, Akita-Shi, Japan*
[2] *Mathematics Department, College of Engineering and Physical Sciences, Aston University, Birmingham B4 7ET, United Kingdom*
[3] *School of Engineering, Aristotle University, Thessaloniki 54124, Greece; Michigan Technological University, Houghton, MI 49931, USA; Friedrich-Alexander-University at Erlangen-Nurember, 90762 Fürth, Germany*

Received March 29, 2023; revised April 10, 2023; accepted May 14, 2023

Abstract—In this study systematic numerical analyses are outlined searching for additional instabilities in the co-rotating Taylor–Couette system within the fully deterministic sequential approach of bifurcations (SBA) to turbulence. The main idea of the search strategy is the application of a forcing function, rotation, which has a direct physical interpretation, and that was realized in prior experimental work. The forcing induces disturbances that lead to bifurcations of new states. Thus, turbulence can be generated and observed in a rotating fluid without the imposing additional forcing sources. The imposition of thermoconvective forcing in the Taylor–Couette system will be discussed separately. Important findings include the discovery of the interplay of new and already known states, the transition of steady states to oscillatory ones and higher order states in the SBA via vortex merger/separation and re-allocation of symmetries for a more intensified mass transport. The results of the present work enhance the results of [1]. They will be revisited within an internal length gradient (ILG) framework accounting for weekly nonlocal effects as suggested in the concluding section of the paper.

2010 Mathematical Subject Classification: 76A05, 76Dxx, 70K30, 70K50

Keywords and phrases: *Incompressible flow, Bifurcation theory, strongly nonlinear solution, stability theory, bifurcation theory, turbulence, Floquet parameters, Taylor–Couette flow*

1. INTRODUCTION

In the study of the transition from laminar to turbulent flow, the simplest case arises when one can find linear instability modes serving as a first step of a cascade involving more and more complicated dynamics. The corresponding theory has a long history resting on linear stability analysis of parallel flows, as described, e.g., by [2]. A cornerstone of the approach was Squire's theorem stating that most unstable modes are slantwise uniform. In this manuscript our formulation which extends the results of [1], employs a numerical collocation method in the wall coordinate through the Gauss–Lobatto procedure points and Fourier transforms in the other coordinates for the Taylor–Couette system under consideration.

The problem of three-dimensional flows arising from the twist instability of Taylor vortices is investigated experimentally in the finite gap limit of the Taylor–Couette system with nearly corotating cylinders in [3]. In this paper we study numerically the same system but in the narrow

* E-mail: akinagat@gipc.akita-u.ac.jp
** E-mail: s.c.generalis@aston.ac.uk
*** E-mail: mom@mom.gen.auth.gr

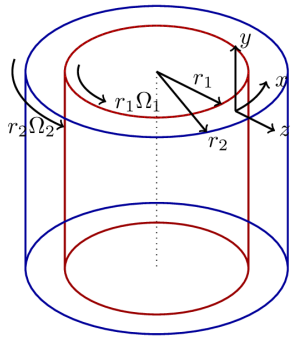

Figure 1. The geometrical configuration of the system studied in [3]. Circular Taylor–Couette system: two co-axial cylinders of radii r_1 and r_2, rotating with different speeds $\Omega_1 r_1$ and $\Omega_2 r_2$, respectively. The system is rotating with angular velocity $\mathbf{\Omega}(=(0,\Omega,0))$ and the two plates are drifting with a relative velocity $2U$ in x direction. The gap width between the two infinite plates is $2h$ (non-dimensional parameters). The x, y and z coordinates correspond to the azimuthal, axial and radial directions, in the narrow gap approximation of the circular Taylor–Couette system, employed in our analysis respectively.

gap approximation based on the Navier–Stokes equations. In particular, the nonlinear solutions are obtained from a harmonic analysis based of the dimensionless Navier–Stokes equations and the sequence of bifurcations method is employed via incorporating a linear stability analysis of the nonlinear states. The theoretical findings are compared with experimental observations and the stability diagrams of [3], for the parameter range of the experiment. The stability range is characterized by the two types of twist vortices: those that do not deform the in- and outflow boundaries of the Taylor vortices and those that do. The latter type are called wavy twist vortices and correspond to class I1 of [4], with the result that the twist solutions are unstable within a large range of the parameter space with respect to Eckhaus and skewed-varicose-type instabilities. These tertiary states are re-examined and their stability ranges are compared with experiment. We extend the stability bifurcation sequence up to and including quaternary and quinary order states, where good agreement with experiment is shown for a certain region of the parameter space. In the case, where departure between theory and experiment occurs, an explanation for the disagreement is provided.

Apart from Rayleigh–Bénard convection, Taylor–Couette flow between almost co-rotating cylinders is the best known system for the study of transitions of shear flow from laminar to more complex forms of fluid motion. Because of the particular direction of the axis of rotation and because of the different radii of the cylinders the Taylor–Couette system exhibits fewer symmetries than a horizontally extended Rayleigh–Bénard layer with a Boussinesq fluid. In the limit of a small gap between the two coaxial cylinders an additional symmetry is gained, however, and the Taylor–Couette system becomes equivalent with respect to its symmetries to a Rayleigh–Bénard layer of an electrically conducting fluid with an imposed horizontal magnetic field, for instance. In fact, the two-dimensional rolls, which are the preferred mode at the onset of instability, and the Taylor vortices represent mathematically identical solutions of the basic equations if the temperature of the Rayleigh–Bénard layer is identified with the azimuthal velocity field of the Taylor–Couette system and if the Prandtl number is set equal to unity.

The basic equations are formulated and discussed in Section 2, where the nomenclature for the SBA states is also listed. In Section 3, the methodology used for the numerical solutions of the governing equations is discussed. As has been demonstrated by HBA, the properties of solutions bifurcating from axisymmetric Taylor vortices and from tertiary solutions depend rather strongly on the basic wavelength of the vortices. Hence in Section 4 we outline the SBA towards the turbulent regime and provide the stability boundaries for the neighborhood of a selected wave number for the Taylor vortices. Our conclusions are given in Section 5, where a proposal for revisiting these results within a more general setting employing higher order velocity gradients is outlined.

2. MATHEMATICAL FORMULATION OF THE PROBLEM

We consider the flow in the narrow gap between two coaxial cylinders with radii r_1 and r_2 that are rotating with speeds $\Omega_1 r_1$ and $\Omega_2 r_2$, respectively. The gap width $2d \equiv r_2 - r_1$ will be used as

length scale in the following and d^2/ν as timescale, where ν is the kinematic viscosity of the fluid. We introduce a Cartesian system of coordinates with the z-coordinate in the radial direction, the x-coordinate in the azimuthal direction and the y-coordinate in the direction of the axis as shown in Fig. 1. The corresponding unit vectors will be denoted by $\boldsymbol{k}$, $\boldsymbol{i}$, $\boldsymbol{j}$. The dimensionless Navier–Stokes equations can then be obtained in the form [1]

$$\left(\frac{\partial}{\partial t}+\boldsymbol{u}\cdot\nabla\right)\boldsymbol{u}+\Omega\,\boldsymbol{j}\times\boldsymbol{u}=\,-\nabla\pi+\nabla^2\boldsymbol{u},\qquad \nabla\cdot\boldsymbol{u}=0, \tag{1}$$

where $\boldsymbol{u}$ denotes the velocity, π is the pressure and Ω is twice the mean rotation rate in dimensionless units, $\Omega=(\Omega_1+\Omega_2)\,d^2/\nu$.

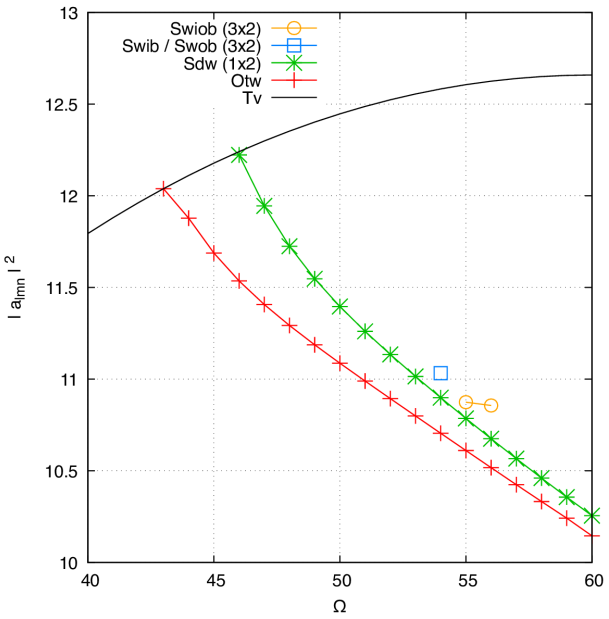

Figure 2. Pattern competition through to quinary level: $|a_{lmn}|^2$ represents the ℓ^2_{norm} [1], which is a measure of the strength of the flow. Here the bifurcations of the secondary to quinary states are indicated for $\beta=\beta_0/2$ and $\alpha=\beta_0/3$ for the quaternary Swib/Swob and for the quinary Swiob respectively. For the tertiary Sdw $\alpha=1.875, \beta=\beta_0/2$, where $\beta_0=1.25$ is the wave number of the secondary Tv.

The boundary conditions are given by $\boldsymbol{u}=\mp R\boldsymbol{i}\quad$ at $\quad z=\pm1$, where the Reynolds number R is defined by $R\equiv(\Omega_1-\Omega_2)\,(r_1+r_2)\,d/(4\nu)$.

It is convenient to dispense with the equation of continuity by the introduction of the following general representation of the velocity field

$$\boldsymbol{u}=\,(-Rz+U(t,z))\,\boldsymbol{i}+V(t,z)\boldsymbol{j}+\widetilde{\boldsymbol{u}},\qquad \widetilde{\boldsymbol{u}}=\nabla\times(\nabla\times\boldsymbol{k}\phi)+\nabla\times\boldsymbol{k}\psi. \tag{2}$$

By using the operators $\boldsymbol{k}\cdot\nabla\times(\nabla\times\ldots,)$ and $\boldsymbol{k}\cdot\nabla\times$ on Eqs. (1), we obtain the following two equations for ϕ and ψ

$$\left(\nabla^2-\frac{\partial}{\partial t}\right)\nabla^2\triangle_2\phi-\Omega\frac{\partial}{\partial y}\triangle_2\psi=(-Rz+U)\,\frac{\partial}{\partial x}\nabla^2\triangle_2\phi-\frac{\partial^2U}{\partial z^2}\frac{\partial}{\partial x}\triangle_2\phi$$
$$-\frac{\partial^2V}{\partial z^2}\frac{\partial}{\partial y}\triangle_2\phi+V\frac{\partial}{\partial y}\nabla^2\triangle_2\phi+\boldsymbol{k}\cdot\nabla\times(\nabla\times(\widetilde{\boldsymbol{u}}\cdot\nabla\widetilde{\boldsymbol{u}}))\,,$$

Table 1. Nomenclature for the SBA states in the Taylor–Couette system for the present study. We note that the subharmonic wavy inflow/outflow boundary states were reported as tertiary states in [4].

SBA Order	States	Short names
Secondary	Taylor vortex flow	Tv
Tertiary	Ordinary twists (Twist vortices)	Otw
	Subharmonic drifting wavy vortex	Sdw
Quaternary	Oscillatory Ordinary twists (Twist vortices)	Ootw
	Subharmonic wavy inflow boundary/	Swib
	Subharmonic wavy outflow boundary	Swob
Quinary	Subharmonic wavy	Swiob
	inflow-outflow boundary	

$$\left(\nabla^2 - \frac{\partial}{\partial t}\right) \triangle_2\psi + \Omega\frac{\partial}{\partial y}\triangle_2\phi = (-Rz + U)\,\frac{\partial}{\partial x}\triangle_2\psi + \left(R - \frac{\partial U}{\partial z}\right)\frac{\partial}{\partial y}\triangle_2\phi + V\frac{\partial}{\partial y}\triangle_2\psi + \frac{\partial V}{\partial z}\frac{\partial}{\partial x}\triangle_2\phi - \boldsymbol{k}\cdot\nabla\times(\widetilde{\boldsymbol{u}}\cdot\nabla\widetilde{\boldsymbol{u}})\,,$$

and the following two equations for the mean flows in the azimuthal and axial directions respectively

$$\left(\frac{\partial^2}{\partial z^2} - \frac{\partial}{\partial t}\right) U = -\frac{\partial}{\partial z}\overline{\triangle_2\phi\left(\frac{\partial^2}{\partial x\partial z}\phi + \frac{\partial}{\partial y}\psi\right)}, \tag{3}$$

$$\left(\frac{\partial^2}{\partial z^2} - \frac{\partial}{\partial t}\right) V = -\frac{\partial}{\partial z}\overline{\triangle_2\phi\left(\frac{\partial^2}{\partial y\partial z}\phi - \frac{\partial}{\partial x}\psi\right)}. \tag{4}$$

The time dependence of the mean components has been neglected, since we are interested in flow states that exist under steady external conditions. We note here that U, V are the mean flows in the azimuthal (x) and axial (y) directions, respectively. Note that the mean flow V (for the axial direction), was not considered in [5], in contrast to the present study, where the mean flows in both directions are being considered.

The mean flow equations over the axial and azimuthal directions are obtained when the velocity components are averaged over surfaces $z = const$ (this average is indicated by a bar) and the operator $\triangle_2$ is defined by $\triangle_2 \equiv \nabla^2 - (\boldsymbol{k}\cdot\nabla)^2$.

The appropriate boundary conditions are

$$\phi = \frac{\partial\phi}{\partial z} = \psi = U = V = 0 \qquad \text{at} \qquad z = \pm 1.$$

3. HARMONIC EXPANSION

We assume periodicity in stream-wise (x) and span-wise (y) directions, whereas the non-slip boundary conditions at the boundaries in the wall coordinate are assumed (z). For the poloidal (ϕ)

and toroidal (ψ) parts of Eqs. (2), we assume the following expansions [1]

$$\phi\left(x,y,z\right)=\sum_{\ell=0}^{L}F_{\ell}(z)\widehat{\phi}_{\ell},\quad \psi\left(x,y,z\right)=\sum_{\ell=0}^{L}G_{\ell}(z)\widehat{\psi}_{\ell},$$

where

$$\widehat{\phi}_{\ell}=\sum_{(m,n)\neq(0,0)}^{|m|\leq M,|n|\leq N}a_{\ell mn}\exp\left\{\mathrm{i}\left[m\alpha\left(x-ct\right)+n\beta y\right]\right\},$$

$$\widehat{\psi}_{\ell}=\sum_{(m,n)\neq(0,0)}^{|m|\leq M,|n|\leq N}b_{\ell mn}\exp\left\{\mathrm{i}\left[m\alpha\left(x-ct\right)+n\beta y\right]\right\},$$

which c denoting the phase speed, in order to also take into account shape preserving traveling wave solutions. The following equations were used for the mean flows in the azimuthal and axial directions [1]

$$U\left(z\right)=\sum_{\ell=0}^{L}F_{\ell}(z)\;c_{\ell},\quad V\left(z\right)=\sum_{\ell=0}^{L}G_{\ell}(z)\;d_{\ell}+\mu\left(z^{2}-1\right),$$

where μ is determined by the condition of vanishing mass flux in the y-direction,

$$\int_{-1}^{+1}V(z)\,dz=0,$$

thus ensuring that the numerical model is a true reflection of the experimental set-up of [3]. The integer values L,M,N are the predetermined truncation levels and $a_{\ell mn},b_{\ell mn},c_{\ell},d_{\ell}$ are constants to be determined. The truncation levels have to be sufficiently high such that the nonlinear solutions do not change significantly if L,M,N are increased. In our studies a typical set of truncation levels for the reported tertiary states with $L=13,M=8,N=13$ were generally sufficient. For states from subharmonic instability $2:1$ and $3:1$ the double and triple truncation levels must be selected, respectively. This inevitably results in a large number of coefficients $a_{\ell mn},b_{\ell mn},c_{\ell}$ and d_{ℓ} from Eqs. (3) and (4), that need to be determined. We can reduce the number of coefficients to be calculated by using relationships such as

$$a_{\ell-m-n}=a_{\ell mn}^{*}a_{\ell m0}^{*},\quad a_{\ell0-n}=a_{\ell0n}^{*},\quad\cdots,$$

These result from the conditions $\phi=\phi^{*}$ and $\psi=\psi^{*}$, where ϕ^{*},ψ^{*} refer to the complex conjugate of ϕ,ψ, respectively. Additionally equations that refer to the symmetries of the nonlinear states that are sought can also be used. This reduces the number of coefficients further and makes the study of the nonlinear solutions, at relatively high truncation levels possible.The quantities $F_{\ell}(z)$ and $G_{\ell}(z)$ $(\ell=0,1,\ldots,L)$ are combinations of the 1st kind Chebyshev polynomials ($T_{\ell}(z)$ $(\ell=0,1,\ldots)$),

$$F_{\ell}\left(z\right)=\frac{\left(\ell+1\right)T_{\ell+4}(z)-2\left(\ell+2\right)T_{\ell+2}(z)+\left(\ell+3\right)T_{\ell}(z)}{4\left(\ell+2\right)},\quad G_{\ell}\left(z\right)=\frac{T_{\ell}\left(z\right)-T_{\ell+2}\left(z\right)}{2},$$

that are employed in order to satisfy

$$F_{\ell}\left(z=\pm1\right)=0,\quad\frac{dF_{\ell}}{dz}\left(z=\pm1\right)=0,\quad G_{\ell}\left(z=\pm1\right)=0.$$

As an example, of the above decomposition of the velocity field in poloidal and toroidal components we can write for $\widetilde{\boldsymbol{u}}$ of Eq. (2), the expression

$$\widetilde{\boldsymbol{u}}=\left(\frac{\partial^{2}\phi}{\partial x\partial z}+\frac{\partial\psi}{\partial y}\right)\boldsymbol{i}+\left(\frac{\partial^{2}\phi}{\partial y\partial z}-\frac{\partial\psi}{\partial x}\right)\boldsymbol{j}-\left(\triangle_{2}\phi\right)\boldsymbol{k}.\tag{5}$$

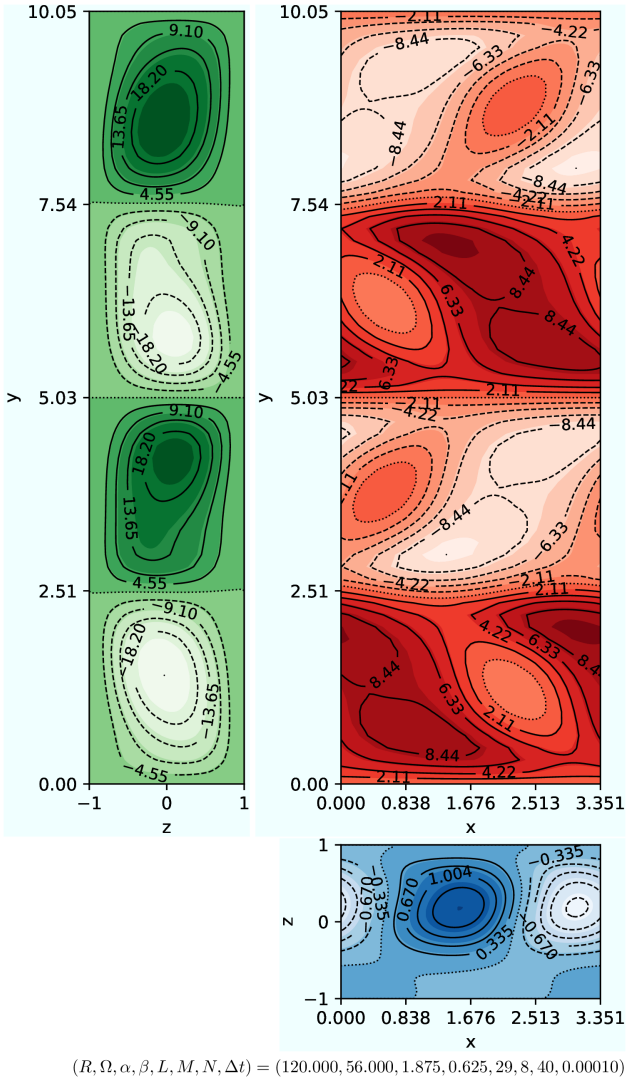

$(R, \Omega, \alpha, \beta, L, M, N, \Delta t) = (120.000, 56.000, 1.875, 0.625, 29, 8, 40, 0.00010)$

Figure 3. Pattern competition at the tertiary and quaternary levels: Sdw at different $\Delta t (= 0.0001, 0.0002)$ for $R, \Omega, \alpha, \beta, L, M, N$ as indicated.

4. SEQUENCE OF BIFURCATIONS-STABILITY ANALYSIS

Most efforts that are directed towards an improved understanding of turbulent fluid flow are based on statistical analysis. Details of the nearly random velocity fields observed in laboratory experiments or in numerical simulations are difficult to capture though and, therefore, one usually tries to characterize turbulent flows by their time averaged properties.

Our goal here is to demonstrate that using Eqs. (3) and (4) solutions of the basic Navier–Stokes equations (NSE) of motion can be quite useful for the understanding of typical dynamical mechanisms operating in turbulent fluid systems and, additionally, make strong contact between theory and experiment. While the spatially and temporally periodic solutions of the NSE do not exhibit the chaotic nature of observed turbulence they may well exhibit the same transport mechanism that also operates under turbulent conditions at high values of the control parameter. These regular solutions as we shall call them, in distinction to the turbulent solutions, may often be unstable and thus not observable in experiments. But there are many situations where regular solutions are stable with respect to infinitesimal disturbances and where their basins of attraction in the solution space are just too small to provide them with a chance to be realized in an experiment. Only if controlled initial conditions are used in experiments it may be possible to enter the appropriate basins of attraction and to realize a regular state at external conditions which ordinarily give rise to a turbulent state.

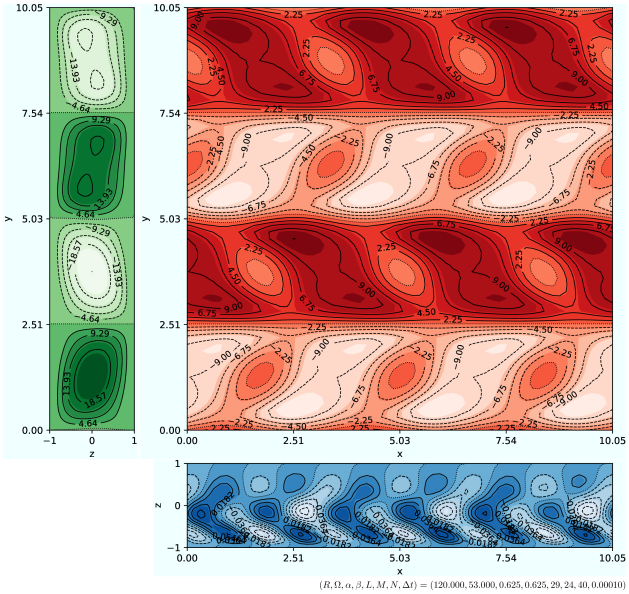

Figure 4. Pattern competition at the tertiary and quaternary levels. The quaternary state Swib/Swob with parameter values as indicated. The characteristic flat surface of the quaternary state is about to acquire curvature indicating that the state is close to the bifurcation point of the quinary state.

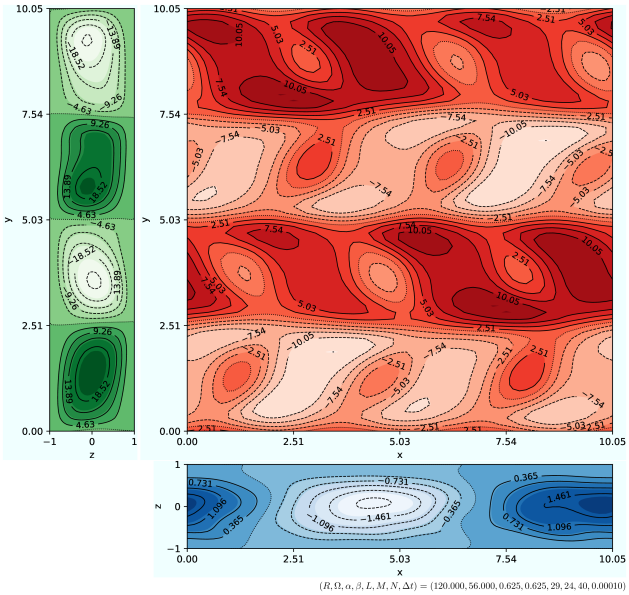

Figure 5. Pattern competition at the quaternary and quinary levels: The quinary state Swiob with parameter values as indicated. Note the double wavy boundary.

The idea of considering regular solutions instead of turbulent states at given external conditions requires the restriction to systems that are homogeneous with respect to at least one dimension in space or in time. Among the manifold of regular solutions only those which are stable with respect to infinitesimal disturbances within a prescribed periodicity interval are of physical interest. In order to make an optimal use of the virtual world of stable regular solutions we shall focus on problems with the maximum number of two homogeneous spatial dimensions and we shall also require homogeneity in time as, for instance, in the case of constant external conditions. Fortunately, these limitations are not overly restrictive since physicists, applied mathematicians and engineers have traditionally studied fluid dynamical problems in their simplest forms which often correspond to a homogeneous configuration.

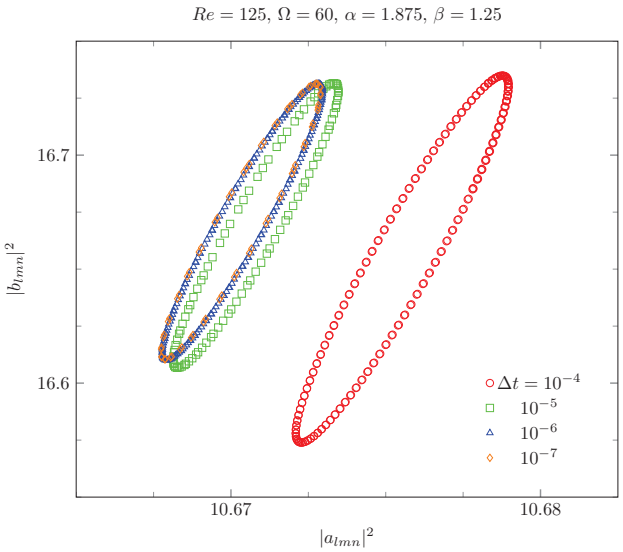

Figure 6. Pattern competition at the tertiary level: Quaternary Oscillatory Ordinary Twist vortices (Ootw): Ootw states are the tertiary Otw states that acquire an oscillatory status for the parameter values as indicated.

In the following we shall point out some typical examples of solutions based on results reported from experimental research. In the process we show that the mechanisms of transition are appropriate for approaching turbulent states in fluid flow. We also explain how new states can be obtained from our simulations via recognizing their symmetry. In this case we can also examine their stability against perturbations via Floquet theory. A set of eigenvalues is obtained with a positive eigenvalue indicating an unstable solution. In the cases where such a procedure is not available the stability boundaries are obtained via a simple change of parameters, until with a particular change of parameters the solution changes to its original state. These are solutions, in general, that cannot be followed in a moving frame, as the solution changes due to its inherent multitude of frequencies, and indicate a prelude to the introduction of a turbulent mechanism. Such stability results and contact with experiment are discussed below.

In order to derive the stability results we superimposed infinitesimal disturbances on the nonlinear solutions using Floquet theory and analysed the stability of the secondary and tertiary states. If we let the infinitesimal disturbances to be of the form

$$\widetilde{\phi}_\ell = \sum_{\ell=0}^{L} F_\ell(z) \sum_{(m,n)\neq(0,0)}^{|m|\leq M,|n|\leq N} \widetilde{a}_{\ell mn} \exp\left\{\mathrm{i}\left[(m\alpha + d)\, x + (n\beta + b)\, y\right] + \sigma t\right\}, \tag{6}$$

$$\widetilde{\psi}_\ell = \sum_{\ell=0}^{L} G_\ell(z) \sum_{(m,n)\neq(0,0)}^{|m|\leq M,|n|\leq N} \widetilde{b}_{\ell mn} \exp\left\{\mathrm{i}\left[(m\alpha + d)\, x + (n\beta + b)\, y\right] + \sigma t\right\}, \tag{7}$$

then the above Floquet ansatz applies for general three-dimensional disturbances since our solutions are periodic in the azimuthal and axial dimensions. Unless $d = b = 0$ is to be considered, then no disturbances to Eqs. (3) and (4) need to be taken into account. Equations (6) and (7) give rise to a linear homogeneous system for the unknowns $\widetilde{a}_{\ell mn}, \widetilde{b}_{\ell mn}$ with the growth rate σ as eigenvalue. For a given stationary (nonlinear) solution (3) and (3) the maximum real part σ_r of σ must be determined as a function of d, b. If this maximum is less or equal to zero (the case when the imposed disturbances (6) and (7) decay) the nonlinear state is stable, otherwise it is unstable. Regions of stable stationary solutions of the form (3), (4) can thus be identified as functions of the external parameters of the problem at hand and of course α, β.

As the imposed disturbances grow to finite amplitude we distinguish the two possibilities: either the asymptotic state corresponds to one of the stationary solutions with different wave number $\boldsymbol{\alpha} = (\alpha, \beta)$, or a three-dimensional, with/without time dependence, solution is realized. The latter

type of new solution is describing a tertiary state that can be analysed by the same numerical method described here, as it bifurcates from the $\sigma_r = 0$ curve.

In our analysis we have also identified solutions of the form

$$\widetilde{\phi}_\ell = \sum_{\ell=0}^{L} F_\ell(z) \sum_{(m,n)\neq(0,0)}^{|m|\leq M,|n|\leq N} \widetilde{a}_{\ell mn} \exp\left\{\mathrm{i}\left[(m\alpha + d)\,(x - ct) + (n\beta + b)y\right] + \sigma t\right\}, \tag{8}$$

$$\widetilde{\psi}_\ell = \sum_{\ell=0}^{L} G_\ell(z) \sum_{(m,n)\neq(0,0)}^{|m|\leq M,|n|\leq N} \widetilde{b}_{\ell mn} \exp\left\{\mathrm{i}\left[(m\alpha + d)\,(x - ct) + (n\beta + b)\,y\right] + \sigma t\right\}, \tag{9}$$

for solutions that are of the traveling wave form.

In this case the phase speed c would need to be determined. Except the geometric method we can evaluate the phase speed independently. In our studies we use a Galerkin-type programme that is capable of following the solution as it moves with a phase speed c. In this case the phase speed is one of the unknowns and is determined explicitly by our numerical method.

Unless the superimposed growing disturbances on a nonlinear solution are of the form of Eqs. (6) and (7), they are determined via a forward time integration technique. Growing disturbances of the form of Eqs. (8) and (9) lead to time dependent flows, as there is no direction for which the flow can be uniform, as in the case of flows bifurcating from *gray*◯ of Fig. 2 for example. In the case of more than one phase speed we have the prelude of existence of aperiodic motion.

5. CONCLUSIONS

In this article we have extended the work of [1], where extensive comparisons were made with the experiments of Andereck and co-workers [3]. Using in house developed software, appropriate modeling of the relevant Navier–Stokes equations can track oscillatory, monotonic or phase locked solutions and, additionally, can locate the stability boundaries of the obtained solutions. Although a particular set of (α, β) wave number values has been selected (so that comparisons with experiments can be direct) results for a variety of rotation and Reynolds number values are also reported complementary. We have therefore identified complementary ways to aid and verify the results of numerical computation. Thus, for the first time the experiments of [3] have theoretical counterparts derived up to and including quaternary states [1] and quinary states. En route to achieving this we have introduced software development that reduces the required computational time, via a combination of physical insight arguments and related mathematical simplifications. In Table 1 we provide the honomatology of the states and their hierarchical status in the SBA approach to turbulence for the Taylor–Couette system. Figure 2 shows this transition, obtained by the methods outlined above.

Moreover, we have provided further evidence that the transition to turbulence via the SBA/Navier–Stokes modeling of the Taylor–Couette system remains a strong realizable possibility. We have shown two routes that the transition to turbulence can take place so that maximum efficiency in mass transport is achieved: that monotonic states can acquire oscillatory status and that flat surfaces can acquire curvature with the offering of the final break-up to hairpins [6]. The road map of the SBA to turbulence for the Taylor–Couette system is ongoing and further results will be reported elsewhere.

5.1. Application of the Gradient Theory and the SBA to the Taylor–Couette system

Turbulent flows exhibit internal structure in the form of hairpins [6]. This suggests that it may be possible to use generalized continuum mechanics theories taking into account submicroscopic features of the flow such as eddies and other spatial inhomogeneities. One effective way to account for these is to introduce nonlinearity in the Navier–Stokes equations by employing the so called internal length gradient (ILG) framework [7, 8]. In the present case of incompressible Newtonian fluids, this amounts to replacing the standard expression for the stress $\boldsymbol{\tau}$ by the weakly non-local gradient expression

$$\boldsymbol{\tau} = -p\mathbf{1} + 2\mu(1 - l_{\boldsymbol{D}}^2\nabla^2)\boldsymbol{D},$$

where $l_{\boldsymbol{D}}$ is an internal length parameter accounting for weakly non-local gradient effects, μ is the viscosity and $\boldsymbol{D}$ the symmetric part of the velocity gradient. The introduction of the Laplacian is not arbitrary, but it arises from a Taylor series expansion of a non-local integral expression for the average (macroscopic) stress which, by retaining terms up to the second order in the Taylor series expansion, is replaced by the local (microscopic) stress and its Laplacian multiplied by the internal length parameter $l_{\boldsymbol{D}}$. The determination of the new phenomenological parameter $l_{\boldsymbol{D}}$ is left to experiments and simulation, and the same holds for the new type of boundary conditions that the Laplacian term requires. Then, the modified, gradient enhanced Navier–Stokes (NS) equations of incompressible flow (see also [10])

$$\rho\frac{D\boldsymbol{u}}{Dt} = -\nabla\pi + \mu(\Delta\boldsymbol{u} - l_D^2\Delta^2\boldsymbol{u}), \tag{10}$$

where $\Delta = \nabla^2$ and $\Delta^2 = \nabla^4$ denote the Laplacian and biharmonic operators respectively. It is noted that Eq. (10) is identical to the equation used to model plane Poiseuille liquid flow at small-length scales as discussed in [8, 9]. Within the framework of ILG and for the one-dimensional flow of the Taylor–Couette system the velocity field has the form $\boldsymbol{u}(\mathbf{x},t) = v(y)\mathbf{e}_{\mathbf{x}}$, where v is the only not vanishing velocity coordinate in direction $\mathbf{e}_x$ and y is the cross-sectional coordinate of the gap. Thereby the velocity v is understood as a quantitative average at a location y over a certain period of time. Then, the constitutive equation for the shear stress τ_{xy} of a fluid follows

$$\tau_{xy} = \kappa_1\frac{dv}{dy} - \kappa_2\frac{d^3v}{dy^3},$$

where κ_1 and κ_2 are material coefficients. The equation of motion degenerates to

$$\kappa_1\frac{d^2v}{dy^2} - \kappa_2\frac{d^4v}{dy^4} = A, \quad A = \frac{d}{dx}(p+U) = \text{ const.}$$

Setting $A = 0$ and using the symmetry condition $v(y) = -v(-y)$ one obtains the general solution $v(\eta) = C_1\eta + C_2\sinh\Gamma\eta$ with arbitrary constants C_1 and C_2 and $\eta = \frac{y}{h/2}$ $,\Gamma = \frac{\lambda \mathrm{h}}{2}$, $\lambda^2 = \frac{\kappa_1}{\kappa_2}$, where λ is a material coefficient. To satisfy the non negative specific dissipation energy κ_1, κ_2 and Γ must be $\kappa_1 \geq 0$, $\kappa_2 \geq 0$, $\Gamma \geq 0$. Herein the constants C_1 and C_2 in (15) are given by [9]

$$C_1 = \frac{(1-\vartheta)\sinh\Gamma + (\omega-\varsigma)\Gamma\cosh\Gamma}{(1+\zeta-\vartheta-\omega\vartheta^2)\sinh\Gamma + (\omega+\omega\zeta-\varsigma-\omega\zeta\vartheta)\Gamma\cosh\Gamma}\mathrm{V},$$
$$C_2 = \frac{\zeta-\omega\vartheta}{(1+\zeta-\vartheta-\omega\vartheta^2)\sinh\Gamma + (\omega+\omega\zeta-\zeta-\omega\zeta\vartheta)\Gamma\cosh\Gamma}\mathrm{V},$$

with

$$\omega = \frac{\lambda_{w'}}{\lambda_{\mathrm{v}}\mathrm{h}/2}, \quad \zeta = \frac{\lambda_{v'v'}}{\lambda_{w'}\mathrm{h}/2}, \quad \vartheta = 1 - \frac{\mu}{\lambda_{\mathrm{w}'}}.$$

We will be reporting work on the numerical verification of the ILG theory adjustments to classical Navier–Stokes equations for the Taylor–Couette problem, including non-linear effects, in the near future.

6. ACKNOWLEDGEMENTS

This work was funded by the RISE-Grant 824022 – ATM2BT of the European H2020-MSCA programme.

REFERENCES

1. T. Akinaga, S. C. Generalis, and F. H. Busse, Tertiary and Quaternary states in the Taylor–Couette system, Chaos Sol. & Fr. **109**, 107–117 (2018).
2. P. J. Schmid and D. S. Henningson, Stability and Transition in Shear Flows. Springer.
3. J. J. Hegseth, G. W. Baxter, and C. D. Andereck, Bifurcations from Taylor vortices between corotating concentric cylinders, Phys. Rev. E **53**, 507–521 (1996).

4. M. Nagata, Bifurcations in Couette flow between almost corotating cylinders, J. Fluid Mech. **169**, 229–250 (1986).
5. E. Weisshaar, F. H. Busse, and M. Nagata, Twist vortices and their instabilities in the Taylor–Couette system, J. Fluid Mech. **226**, 549–564 (1991).
6. T. Itano and S. C. Generalis, Hairpin Vortex Solution in Planar Couette Flow: A Tapestry of Knotted Vortices, Phys. Rev. Lett. **102**, 114501 (2009).
7. E. C. Aifantis, Internal Length Gradient (ILG) Material Mechanics Across Scales and Disciplines, Adv. Appl. Mech. **49**, 1–110 (2016).
8. E. C. Aifantis, Gradient Extension of Classical Material Models: From Nuclear to Condensed Matter Scales to Earth and Cosmological States, E. Ghavanloo et al. (Eds). Size-Dependnet Continuum Mechanics Approaches, Springer Tracts in Mechanical Engineering, Springer Nature Switzerland, AG **2**, 417–452 (2021).
9. G. Silber, R. Trostel, M. Alizadeh, and G. Benderoth, A continuum mechanical gradient theory with applications to fluid mechanics, J. Phys. IV France **8**, 365–376 (1998).
10. E. Fried and M. E. Gurtin, Tractions, balances and boundary conditions for nonsimple materials with application to liquid flow at small-length scales, Arch. Rat Mech. Anal. **182**, 513–554 (2006).